Journal of Nematology 39(2):190–202. 2007.

A New Root-Knot Nematode Parasitizing Sea Rocket from Spanish Mediterranean Coastal Dunes: *Meloidogyne dunensis* n. sp. (Nematoda: Meloidogynidae)

J. E. Palomares Rius,[1] N. Vovlas,[2] A. Troccoli,[2] G. Liébanas,[3] B. B. Landa,[1] P. Castillo[1]

Abstract: High infection rates of European sea rocket feeder roots by an unknown root-knot nematode were found in a coastal dune soil at Cullera (Valencia) in central eastern Spain. Morphometry, esterase and malate dehydrogenase electrophoretic phenotypes and phylogenetic trees demonstrated that this nematode species differs clearly from other previously described root-knot nematodes. Studies of host-parasite relationships showed a typical susceptible reaction in naturally infected European sea rocket plants and in artificially inoculated tomato (cv. Roma) and chickpea (cv. UC 27) plants. The species is herein described and illustrated and named as *Meloidogyne dunensis* n. sp. The new root-knot nematode can be distinguished from other *Meloidogyne* spp. by: (i) perineal pattern rounded-oval, formed of numerous fine dorsal and ventral cuticle striae and ridges, lateral fields clearly visible; (ii) female excretory pore at the level of stylet knobs, EP/ST ratio 1.6; (iii) second-stage juveniles with hemizonid located 1 to 2 annuli anteriorly to excretory pore and long, narrow, tapering tail; and (iv) males with lateral fields composed of four incisures anteriorly and posteriorly, while six distinct incisures are observed for large part at mid-body. Phylogenetic trees derived from distance and maximum parsimony analyses based on 18S, ITS1–5.8S-ITS2 and D2-D3 of 28S rDNA showed that *M. dunensis* n. sp. can be differentiated from all described root-knot nematode species, and it is clearly separated from other species with resemblance in morphology, such as *M. duytsi*, *M. maritima*, *M. mayaguensis* and *M. minor*.

Key words: histopathology, host-parasite relationships, ITS1, ITS2, *Meloidogyne*, morphology, new species, phylogeny, ribosomal DNA, root-knot nematode, scanning electron microscopy, taxonomy.

Sedentary endoparasitic root-knot nematodes of the genus *Meloidogyne* Goeldi, 1892 are among nature's most successful plant parasites, being distributed worldwide and encompassing more than 90 nominal species (Eisenback and Triantaphyllou, 1991; Karssen, 2002; Karssen and Moens, 2006). These nematodes infect thousands of different herbaceous and woody monocotyledonous and dicotyledonous plants and cause serious losses to numerous agricultural crops worldwide (Karssen and Moens, 2006). The systematic position of the genus *Meloidogyne* at family level has been discussed for many years. In this paper, we agree with the classification proposed by De Ley and Blaxter (2002).

Nematode surveys in the Mediterranean coastal sand dunes in central eastern Spain revealed high infection rates of European sea rocket (*Cakile maritima* Scop.) feeder roots by a root-knot nematode. This root-knot nematode is morphologically close related to *Meloidogyne maritima* (Karssen et al., 1998) and resembles *Meloidogyne minor* (Karssen et al., 2004), which prompted us to perform a comparative study among related species. Some reliable diagnostic approaches commonly used to identify and compare certain root-knot nematode species include analyses of isozyme phenotypes and molecular analyses. The analysis of isozyme electrophoretic patterns, in particular esterase (Est) and malate dehydrogenase (Mdh), has been proved to be a valuable tool for precise identification of *Meloidogyne* species (Eisenback and Triantaphyllou, 1991). Similarly, molecular approaches useful for distinguishing *Meloidogyne* spp. include random amplified polymorphic DNA (RAPD) (Blok et al., 1997), restriction fragment length polymorphisms (RFLP) (Hugall et al., 1994) and sequence differences within ribosomal (Wishart et al., 2002; Chen et al., 2003; Blok, 2005) or mitochondrial DNA (Blok et al., 2002). In addition, development of species-specific sequence-characterized amplified region (SCAR) primers has been achieved for rapid identification of the three most widely distributed species, *M. arenaria* (Neal, 1889) Chitwood, 1949, *M. incognita* (Kofoid and White, 1919) Chitwood, 1949 and *M. javanica* (Treub, 1885) Chitwood, 1949 (Zijlstra et al., 2000).

This work describes a new nematode species found infecting European sea rocket and its phylogenetic relationship with other root-knot nematodes based on distance and maximum parsimony analyses of sequences from the 18S, ITS1–5.8S-ITS2 and D2-D3 of 28S rDNA. Additionally, host-parasite relationships were studied in naturally infected European sea rocket and in artificially inoculated tomato (*Lycopersicon esculentum* Mill.) and chickpea (*Cicer arietinum* L.) plants. The undescribed root-knot nematode is herein described as *Meloidogyne dunensis* n. sp., the species epithet referring to the habitat of the nematode.

Materials and Methods

Nematode populations: Samples of European sea rocket roots, together with rhizosphere and bulk soil, were collected with a shovel from the upper 30 cm of soil in Mediterranean coastal sand fore-dunes at Cullera (Va-

Received for publication June 11, 2007.
[1] Instituto de Agricultura Sostenible, Consejo Superior de Investigaciones Científicas (CSIC), Apdo. 4084, 14080 Córdoba, Spain.
[2] Istituto per la Protezione delle Piante, Consiglio Nazionale delle Ricerche (C.N.R.), Sezione di Bari, Via G. Amendola 165/A, 70126 Bari, Italy.
[3] Departmento de Biologia Animal, Biologia Vegetal y Ecología, Universidad de Jaén, Campus "Las Lagunillas" s/n, Edificio B3, 23071-Jaén, Spain.
The authors thank Dr. J.A. Navas Cortés IAS-CSIC for reviewing the manuscript prior to submission and J. Martin Barbarroja and M. León Ropero for technical assistance.
E-mail: ag1cascp@uco.es
This paper was edited by Zafar Handoo.

lencia), central eastern Spain, in December 2005 by the first author. Samples were collected about half way up in the seaward dune face. For diagnosis and identification, females were collected directly from galled roots, while males, eggs and second-stage juveniles (J2) of nematodes were extracted from the rhizosphere by centrifugal-flotation (Coolen, 1979) and from feeder roots of European sea rocket by blending in a 0.5% NaOCl solution for 4 min (Hussey and Barker, 1973). Specimens for light microscopy (LM) were killed with gentle heat, fixed in a 4% solution of formaldehyde + propionic acid and processed to glycerin by Seinhorst's rapid method (Seinhorst, 1966).

To obtain inoculum of *M. dunensis* n. sp. for histopathology and electrophoretic and molecular analyses, the nematode population under study and a reference *M. javanica* population from olive trees sampled at Córdoba, Spain (Nico et al., 2003), were increased on tomato (cv. Roma) in a glasshouse at 25 ± 3°C. For that, a single egg mass of *M. dunensis* n. sp. was placed beneath the roots of individual tomato seedling in 12-cm pots filled with sterile loamy soil. Sixty days after inoculation, tomato plants were uprooted, their roots gently washed free of soil and the root tissues teased apart using forceps and transfer needles to remove adult females. Inoculum for histopathology was obtained by extracting eggs and J2 from 2-mon-old cultures using 0.5% sodium hypochlorite (Hussey and Barker, 1973), followed by centrifugal flotation (Coolen, 1979).

Morphological studies: Individuals (J2 and males) for morphological studies were collected on the rhizosphere and roots of naturally infected European sea rocket as described above. Second-stage juveniles and males were infiltrated in glycerin by standard procedures (Seinhorst, 1966; Esser, 1986). Glycerin-infiltrated specimens were used for studies of morphometric traits and drawings with camera lucida. Photomicrographs of perineal patterns, J2 and males were made with a 35-mm camera attached to a Reichart compound microscope (Reichart-Jung, Milton Keynes, UK) equipped with differential interference contrast (DIC) optics. Measurements of all stages were made with camera lucida and by ocular micrometer. All measurements are in micrometers (μm) unless otherwise stated. Randomly selected specimens of each life-stage were measured. Formaldehyde (4% solution) fixed specimens were dehydrated in a gradient ethanol series, critical-point dried, sputter-coated with gold and observed by scanning electron microscopy (SEM) according to Abolafia et al. (2002).

Perineal patterns of mature females were prepared by standard procedures (Hartman and Sasser, 1985). Briefly, root tissues were teased apart with forceps and half spear to remove adult females. The lip and neck regions of the nematode were excised, and the posterior end was cleared in a solution of 45% lactic acid to remove remaining body tissues. Then, the perineal pattern was trimmed and transferred to a drop of glycerin and processed as described by Hartman and Sasser (1985). At least 50 perineal patterns were examined for species identification.

Isozyme analysis: Esterase and Mdh phenotypes of *Meloidogyne dunensis* n. sp. from Cullera (Valencia), Spain, were compared with a reference population of *M. javanica* from Córdoba, Spain. Five, young egg-laying females of both nematode species were macerated in microtubes containing 5 μL of 20% (wt/vol) sucrose, 1% (vol/vol) Triton X-100 and 0.01% (wt/vol) bromophenol blue. Electrophoresis was carried out in 7 × 8-cm separating (pH 8.8) and stacking (pH 6.8) homogeneous gels, 7% and 4% polyacrylamide, respectively, 0.75-mm thick, with Tris-glycine buffer in a Mini Protean II electrophoresis unit (BioRad, Madrid, Spain). Gels were stained with the substrate α-naphthyl acetate for Est and with Fast Blue RR (Sigma-Aldrich, Madrid, Spain) for Mdh (Esbenshade and Triantaphyllou, 1985).

DNA extraction, PCR assays and sequencing: Nematode DNA was extracted from single adult females. Amplifications were performed with a PTC 200 thermocycler (MJ Research, Watertown, MA). The different regions of rDNA were amplified as described by Castillo et al. (2003) and Tigano et al. (2005) using the following primer sets: MelF (5′-TACGGACTGAGATAATGGT-3′) and MelR (5′-GGTTCAAGCCACTGCGA-3′) for the 18S, 5367 (5′-TTGATTACGTCCCTGCCCTTT-3′) and F195 (5′-TCCTCCGCTAAATGATATG-3′) for the ITS1–5.8S-ITS2, D2A (5′- ACAAGTACCGTGAGGGAAAGTTG-3′) and D3B (5′-TCGGAAGGAACCAGCTACTA-3′) for the D2-D3 region of 28S. The different rDNA products were purified after amplification with a gel extraction kit (Geneclean turbo; Q-BIOgene SA, Illkirch Cedex, France), quantified using a Nanodrop spectrophotometer (Nanodrop Technologies, Wilmington, DE) and used for direct DNA sequencing. DNA fragments from three PCR amplifications from three different samples were sequenced in both directions using the same amplification primers with a terminator cycle sequencing ready reaction kit (BigDye; Perkin-Elmer Applied Biosystems, Warrington, UK) according to the manufacturer's instructions. The resulting products were purified and run on a DNA multicapillary sequencer (Model 3100 genetic analyzer; Applied Biosystems, Foster City, CA) at the University of Córdoba sequencing facilities. The 18S, ITS1–5.8S-ITS2 and D2-D3 sequences of *M. dunensis* n. sp. were deposited as GenBank Accession EF612713, EF612711 and EF612712, respectively.

Phylogenetic analysis: The 18S, ITS1–5.8S-ITS2 and D2-D3 sequences of *M. dunensis* n. sp. were compared directly with sequences in the EMBL and GenBank database using BLAST to identify the most closely related nematode sequences. Database sequences with high similarity were then directly aligned over equalized

lengths with the sequences of *M. dunensis* n. sp. using Bionumerics 4.5 software (Applied Maths, Kortrijk, Belgium). 18S sequence (AJ966499) of *P. thornei* Sher and Allen, 1953 and ITS1–5.8S-ITS2 (AB053485) and D2-D3 (AF170443) sequences of *Pratylenchus coffeae* (Zimmerman, 1898) Filipjev and Schuurmans Stekhoven, 1941 were used as outgroup taxa. Phylogenetic trees were generated by the Neighbor-Joining (NJ) and Maximum-Parsimony (MP) methods with UPGMA cluster analysis using Bionumerics 4.5 software. The phylograms were bootstrapped 1,000 times to assess the degree of support for the phylogenetic branching indicated by the optimal tree for each method.

Histopathology: Galled roots of European sea rocket plants naturally infected by *M. dunensis* n. sp. were selected for histopathological studies. Roots were gently washed free of adhering soil and debris, and individual galls were selected together with healthy roots. Tissues were fixed in formaldehyde chromo-acetic solution for 48 hr, dehydrated in a tertiary butyl alcohol series (40–70–85–90–100%), embedded in paraffin with a melting point of 58°C and sectioned with a rotary microtome. Sections 10–12 µm thick were placed on glass slides, stained with safranin and fast-green, mounted permanently in a 40% xylene solution of a polymethacrylic ester (Synocril 9122X, Cray Valley Products, NJ), examined microscopically and photographed (Johansen, 1940). The same procedures were used for histopathological examination of roots from two cultivated plants, tomato (cv. Roma) and chickpea (cv. UC 27), artificially inoculated with *M. dunensis* n. sp. Both plants were selected since they are a common *Meloidogyne*-susceptible host in temperate and semiarid regions of the Mediterranean Basin.

Systematics

Meloidogyne dunensis n. sp.

(Figs. 1–4, Table 1)

Holotype (female in glycerin): L = 734 µm; maximum body width = 520 µm; a = 1.4; stylet length = 14 µm; dorsal pharyngeal gland opening (DGO) = 4.3 µm; excretory pore from anterior end = 23 µm; excretory pore distance from anterior end/length of stylet (EP/St) = 1.6; vulva slit length = 21 µm; and distance from vulva to anus =14 µm.

Female paratypes: (n = 12) L = 549 ± 86 (395–620) µm; maximum body width = 400 ± 80 (380–542) µm; a = 1.3 ± 0.3 (1.0–1.6); stylet length 14 ± 1.8 (13–16) µm; excretory pore distance 23 ± 1.3 (19–24) µm; EP/ST ratio (excretory pore to anterior end distance/stylet length) = 1.6 ± 0.2 (1.2–1.8); vulva slit = 20 ± 1.2 (18–22) µm; vulva-anus distance = 15 ± 0.8 (13–16) µm.

Female: Body completely or partially enclosed by galled tissue, distinctly annulated, pearly white, pear shaped and sometimes globose. Neck region distinct, 124 ± 5.7 (118–132) µm long. Head region set off from the body, often twisted. Head cap distinct, variable in shape, labial disk elevated; cephalic framework weakly sclerotized. Stylet cone slightly curved ventrally, shaft cylindrical, knobs rounded and sloping backwards in most of the specimens. Excretory pore located slightly posterior to the level of stylet knobs. Pharyngeal gland with a large mononucleate dorsal lobe and two subventral gland lobes. Perineal pattern rounded-oval (as illustrated in figures), typically formed of numerous fine dorsal and ventral cuticle striae and ridges, lateral fields clearly visible. The dorsal arch encloses the usually fine but distinct phasmids. The vulva slit is centrally located to the unstriated area, slightly wider than the vulva-anus distance; anus fold clearly visible. Commonly, large egg sac occurs outside the root gall, containing up to 400 eggs.

Eggs: Embryonated eggs (n = 30): Length: 98 ± 2.8 (94–103) µm; maximum width 40 ± 1.3 (38–42) µm Length/Width = 2.4 ± 0.1 (2.2–2.5). Egg shell hyaline and unsculptured when observed under light microscope. Second-stage juvenile in full embryonated eggs folded three to four times.

Male: Body vermiform, tapering anteriorly; tail rounded, with twisted posterior body portion. Lip region slightly set off, 5.7 ± 0.48 (4.7–6.0) µm high, 11.3 ± 1.16 (8–12.3) µm wide, with large labial annulus and a prominent post labial annulus. Prominent slit-like amphidial openings between labial disc and lateral lips. Labial framework strongly sclerotized; vestibule extension distinct. Stylet with straight cone and shaft. Stylet knobs rounded and sloping backwards. Body annulation distinct, 3 ± 0.4 (2.2–3.7) µm wide. Lateral field composed of four incisures anteriorly and posteriorly. Six distinct incisures were observed at mid-body, forming five equidistant bands, in 20% of the specimens. In SEM (face view), labial disc is high and narrower than the head region, continuous with medial lips; lateral lips absent; stomatal opening slit-like, located in large elongate prestoma. Amphidial apertures large, elongated, slit-like between labial disc and lateral sectors of head region. Testis single, long, monorchic, occupying 31 to 67% of body cavity. Tail usually curved ventrally, short, with bluntly rounded tip and finely annulated. Phasmids small and located at level of the cloaca.

Second-stage juveniles: Body translucent white, vermiform, rather long, tapering at both ends with very long, narrow tail. Anterior end angular; lip region continuous with body contour. In SEM view, the slit-like stoma is located in oval-shaped prestoma, surrounded by six pore-like openings of inner labial sensilla. Medial lips and labial disc dumbbell-shaped in face view. Labial disc rounded, raised slightly above medial lips. Lateral lips small and oval-rounded, lower than labial disc and medial lips. Elongate amphidial apertures located between labial disc and lateral lips. Lip region not annulated; body annuli distinct but fine. Lateral fields be-

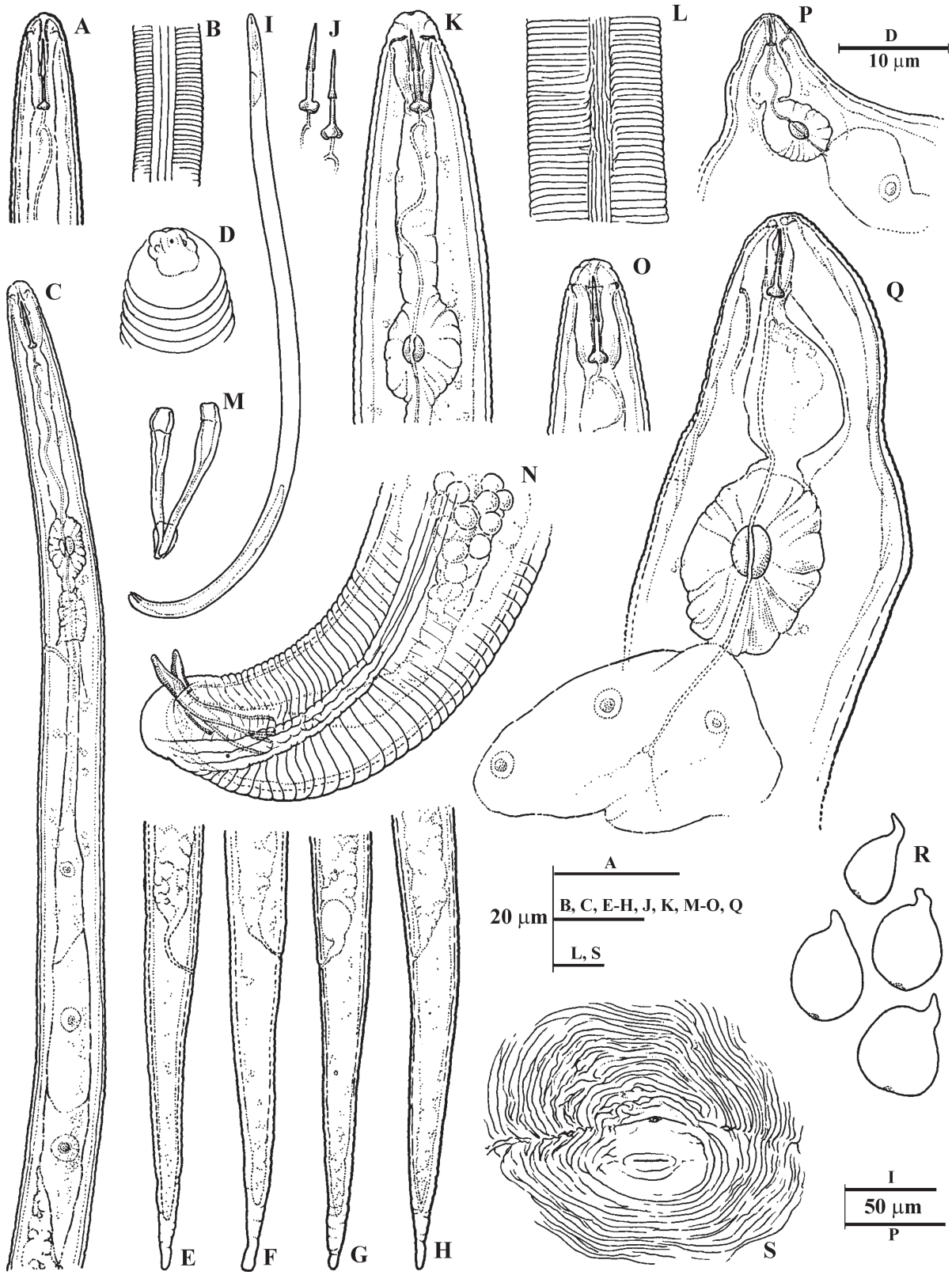

FIG. 1. Line drawings of *Meloidogyne dunensis* n. sp. A) Second-stage juvenile (J2) anterior end. B) J2 lateral field at mid-body. C) J2 pharyngeal region. D) J2 lip region. E-H) J2 tail regions. I) Male entire body. J) male stylet. K, O) Male anterior end. L) Male lateral field at mid-body. P, Q) Female pharyngeal region. R) Outline of whole females. S) Perineal pattern.

ginning near level of procorpus as two lines; near metacorpus third line begins and shortly splits making four lines, running entire length of body until end near hyaline tail terminus, irregularly areolated. Stylet delicate; cone straight, narrow, sharply pointed; shaft becomes slightly wider posteriorly; knobs large, rounded, sepa-

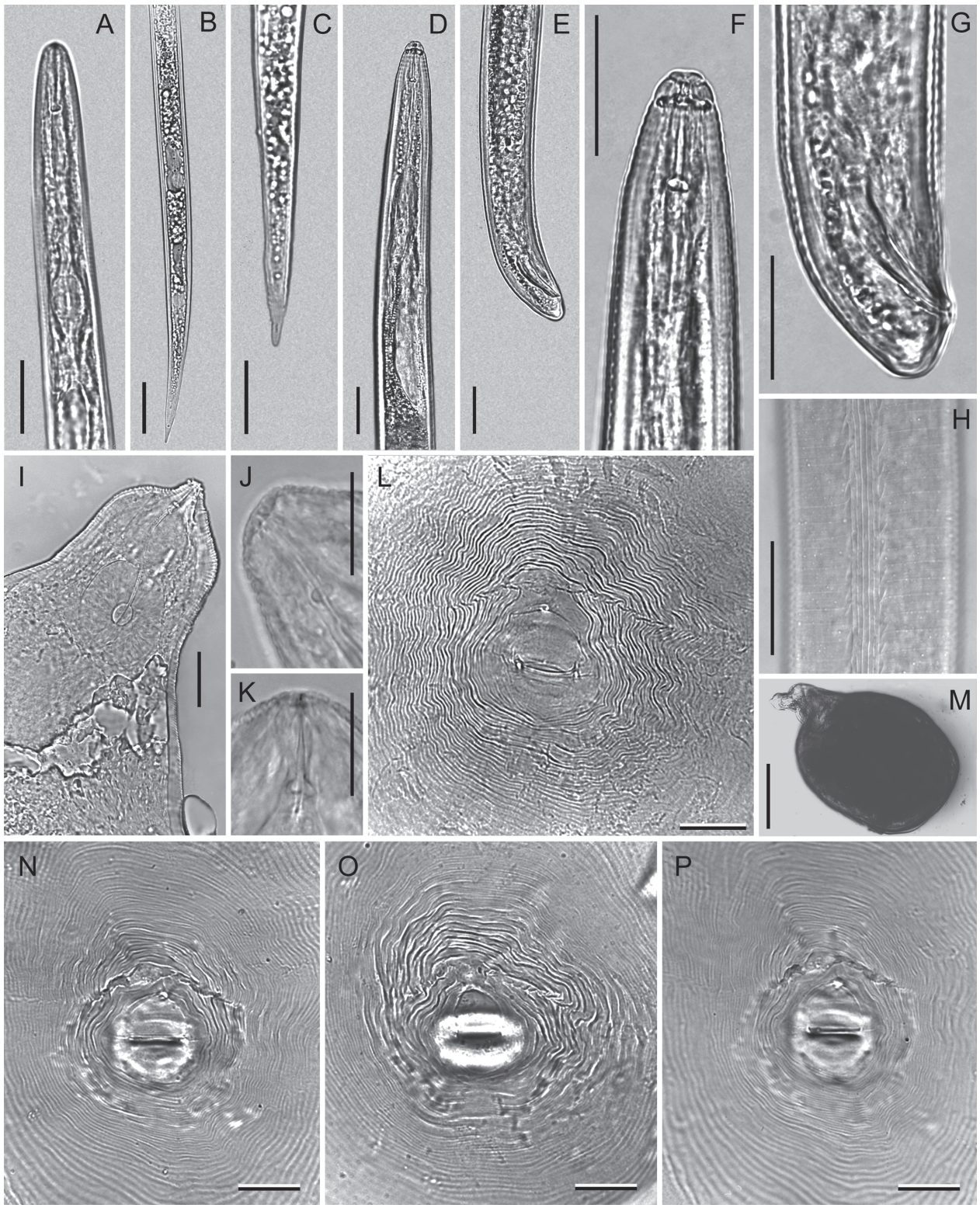

FIG. 2. Photomicrographs of *Meloidogyne dunensis* n. sp. Second-stage juvenile (A-C): A) Pharyngeal region. B, C) Tail regions. Male (D-H): D) Pharyngeal region. E, G) Tail region at different magnification. F) Lip region. H) Lateral field. Female (I-P): I) Pharyngeal region. J, K) Anterior end. L, N-P) Perineal patterns. M) Whole body. Scale bars: A-I, L, N-P = 25 µm; J, K = 15 µm. M = 250 µm.

rate from each other, backwards directed. Procorpus faintly outlined; metacorpus oval-shaped with enlarged lumen lining; isthmus not clearly defined, pharyngeal-intestinal junction at excretory pore level, or slightly anterior to it. Gland lobe variable in length, with three equally sized nuclei and overlapping intestine ventrally. Excretory pore distinct, at level with the half or posterior third of isthmus. Hemizonid distinct, located 1 to 2

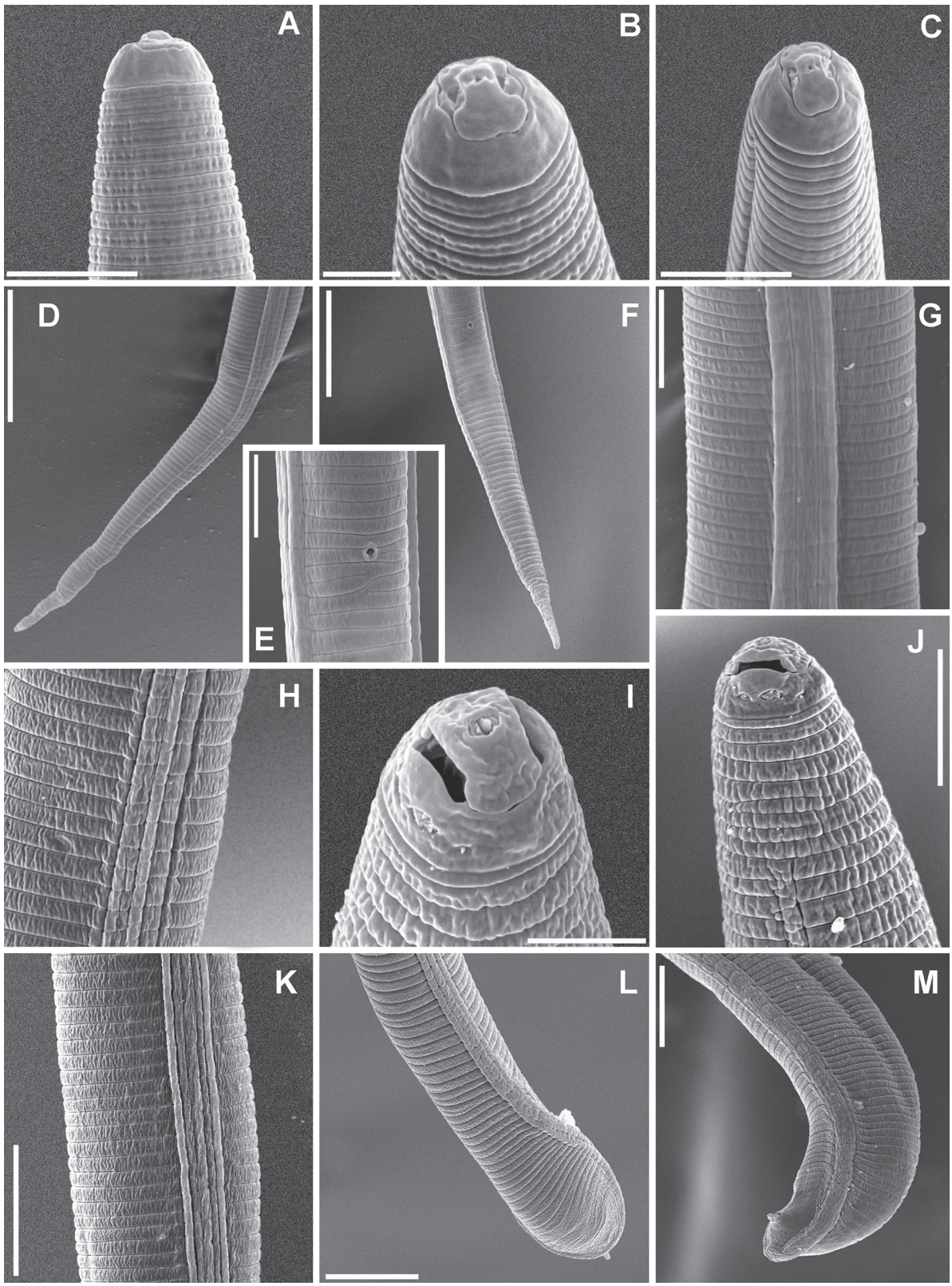

FIG. 3. Scanning electron microscope photographs of *Meloidogyne dunensis* n. sp. Second-stage juvenile: A-C) Lip region. D, F) Tail region. E) Ventral view of anal region. G, H) Lateral field at mid-body. Male: H) Lateral field at pharyngeal region. I-J) Lip region. K) Lateral field at mid-body. L-M) Tail region. Scale bars: A, C, E, G, I = 5 µm; B = 2 µm; D, F, L, M, 20 µm; H, J, K = 10 µm.

annuli anteriorly to excretory pore, extending for two additional body annuli. Tail thin, conoid; annulations diminish in size, become more irregular posteriorly. Hyaline tail terminus clearly defined; tail tip finely rounded, rarely clavate. Rectum dilated. A few fat droplets may occur in hyaline tail terminus. Phasmids small,

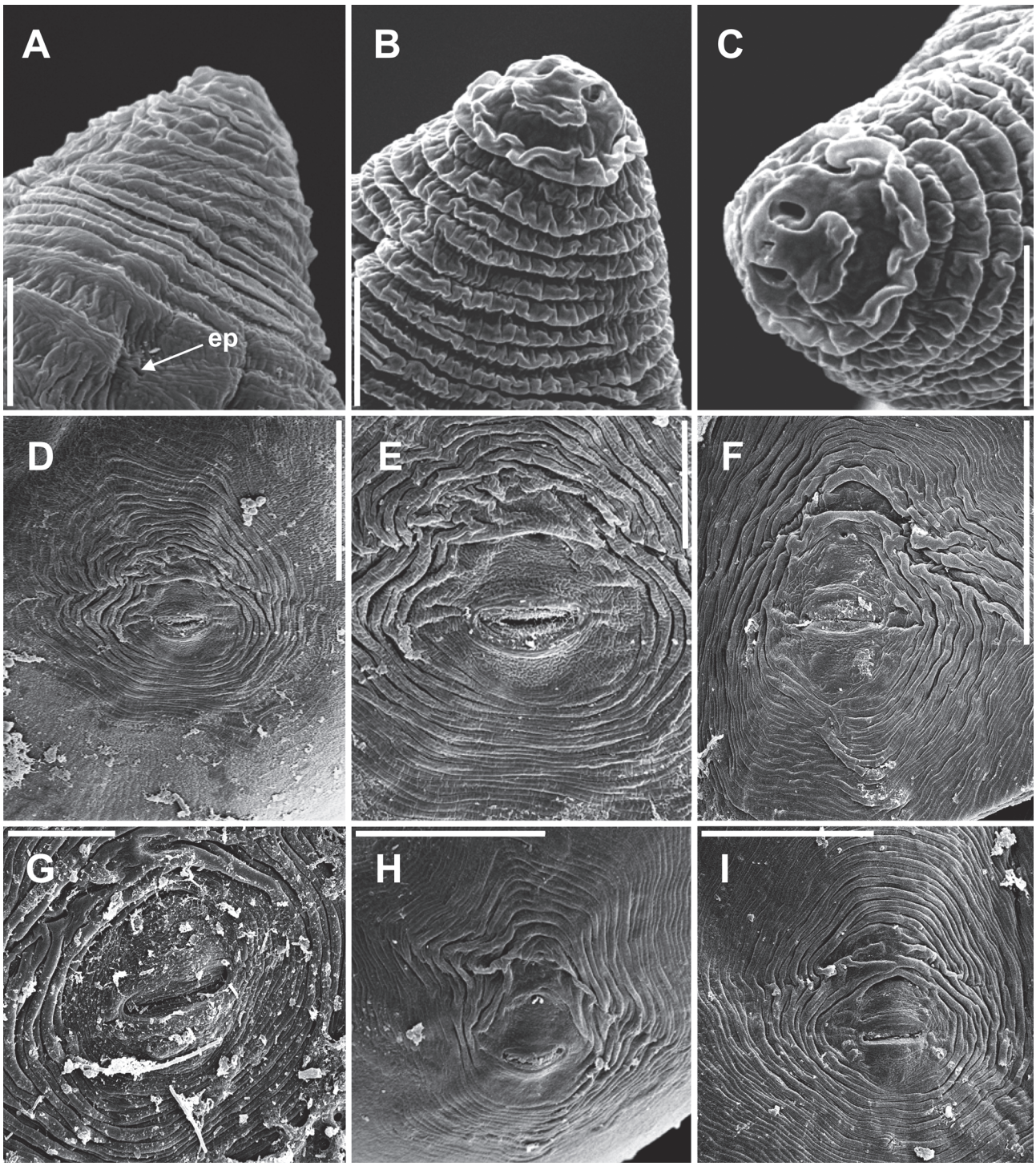

FIG. 4. Scanning electron microscope photographs of *Meloidogyne dunensis* n. sp. A-C) Female lip regions. D-I) Perineal patterns showing typical variation. (ep = excretory pore). Scale bars: A-C = 5 µm; D, F, I = 50 µm; E, G, H= 20 µm.

difficult to observe, located posterior to anus, at mid-tail level.

Type host and locality: Holotype female and additional paratypes from a population extracted from soil samples and infected roots of European sea rocket (*Cakile maritima* Scop.) collected by the first author from the Mediterranean coastal dunes in Cullera (Valencia), central eastern Spain.

Type specimens: Holotype female, female perineal patterns, allotype male, J2 and paratype males, mounted on glass slides deposited in the author's nematode collection at the Istituto per la Protezione delle Piante, CNR, Bari, Italy, and Instituto de Agricultura Sostenible, CSIC, Córdoba, Spain. Additional males and J2 paratypes were distributed to the United States Department of Agriculture Nematode Collection, Belts-

TABLE 1. Morphometrics of adult males and second-stage juveniles (J2) of *Meloidogyne dunensis* n. sp.[a]

	Males	J2
	Mean ± SD (range)	Mean ± SD (range)
n	12	15
L[b]	1,371 ± 172.2 (1,196–1,813)	446 ± 23.0 (417–483)
Head width	11.3 ± 1.2 (8–12.5)	6.0 ± 0.3 (5.5–6.0)
Head height	5.7 ± 0.5 (4.5–6)	2.5 ± 0.2 (2.5–3.0)
Stylet	20 ± 1.6 (16–22)	11.5 ± 0.6 (11.0–12.5)
Conus	11 ± 0.8 (9.5–11.5)	6.0 ± 0.5 (5.0–6.5)
Knobs width	4.5 ± 0.3 (4–5)	2.0 ± 0.3 (2–3)
D.G.O.	3.5 ± 0.7 (2.5–4.5)	2.5 ± 0.4 (1.5–3.0)
O (%)	17.4 ± 3.7 (12.5–24.5)	21.0 ± 3.8 (14–27)
Head to center of median bulb	82 ± 5.5 (74.5–93.0)	58 ± 3.4 (53–56)
Median Bulb height	21.5 ± 2.6 (19.5–26.5)	13 ± 0.9 (12.5–15.0)
Median Bulb width	12.0 ± 1.7 (9.0–14.5)	9 ± 0.6 (8–10)
Isthmus length	22.5 ± 6.9 (12.0–32.5)	—
Pharynx (to cardia)	124 ± 11.5 (108–143)	83 ± 4.3 (77–90)
Pharynx. (to end of gland lobe)	248 ± 63.8 (190–407)	201 ± 23.7 (152–232)
Pharyngeal overlap	124.5 ± 62.6 (59.5–286)	115 ± 23.5 (65–146)
Head end to excretory pore	146 ± 12.2 (121.5–166)	85 ± 4.5 (79–94)
Max body diam.	45 ± 4.0 (36–49)	15.0 ± 1.1 (13–17)
Annuli width	3.0 ± 0.4 (2.2–3.7)	1.1 ± 0.1 (1.0–1.2)
Lateral field width	—	5.0 ± 0.6 (3.5–5.5)
Head end to gonad primordium	—	255 ± 44.2 (184–318)
Testis length	697 ± 183.4 (486–1,057)	—
T (%)	50 ± 12.1 (31–67)	—
Tail length	5.7 ± 1.3 (3.5–8.0)	68.0 ± 7.8 (54–82)
Anal body diam.	17.5 ± 1.9 (14.0–19.5)	11.0 ± 0.8 (9.5–12.5)
Tail hyaline portion (J2)	—	14.0 ± 1.9 (9.5–16.5)
Spicules	35.5 ± 2.9 (29–38)	—
Gubernaculum	8.5 ± 1.3 (6.0–10.5)	—
a	33.4 ± 4.0 (26.8–41.6)	29.5 ± 2.9 (25.6–34.5)
b	11.6 ± 1.4 (9.8–14.9)	5.3 ± 0.3 (4.9–6.0)
b′	5.9 ± 1.1 (4.4–8.0)	2.2 ± 0.3 (2.0–3.0)
c	280.6 ± 59.5 (186.6–385.3)	6.7 ± 0.8 (5.1–8.3)
c′	0.3 ± 0.1 (0.2–0.5)	6.3 ± 0.5 (5.1–6.8)

[a] All measurements are in µm unless otherwise stated.
[b] All other abbreviations used are defined by Siddiqi (2000).

ville, MD, University of California Riverside Nematode Collection and Nematode Collection of Wageningen, Wageningen University and Research Center, Laboratory of Nematology, Wageningen, The Netherlands.

Etymology: The species name is in accordance with the habitat (coastal dunes).

Diagnosis: Meloidogyne dunensis n. sp. can be distinguished from all other *Meloidogyne* spp. by a number of morphological and molecular characteristics. Useful diagnostic characters include the morphology of female perineal pattern, rounded-oval, typically formed of numerous fine dorsal and ventral cuticle striae and ridges; lateral fields not clearly visible in most of fixed specimens; the female excretory pore position, which is slightly posterior to the level of stylet knobs, EP/ST ratio = 1.6 ± 0.2 (1.2–1.8); the second-stage juvenile's body length, which is 417–483 µm long, having a relatively short stylet, 11–12.5 µm in length; the narrow tail, about 70 µm long, tapering to a slender terminal digitiform process, with hyaline region = 14 ± 1.9 (9.5–16.5) µm long; and males with stylet 20 µm long and lateral fields composed of four or rarely six incisures.

Relationships: The female perineal pattern morphology of *M. dunensis* n. sp. places it in the Jepson's Group 3 (Jepson, 1987) and apparently resembles *M. duytsi* Karssen, van Aelst and van der Putten, 1998, *M. maritima* Jepson, 1987, *M. mayaguensis* Rammah and Hirschmann, 1988 and *M. minor*, but differs distinctly from these species in the position of the excretory pore (EP/ST ratio, 1.6 vs. 2.8, 1.1, 3.0 and 1.3, respectively) and perineal pattern morphology. In addition, the following characters and morphometrics separate *M. dunensis* n. sp. from *M. maritima* (Karssen et al., 1998) (Table 2): position of hemizonid in J2 (anterior, adjacent to excretory pore vs. posterior not adjacent to excretory pore), J2 stylet length (11.5 µm vs. 12.4 µm); spicules and gubernaculum length (35, 8.5 µm vs. 28.9, 7.3 µm). Also, *M. dunensis* n. sp. can be differentiated from *M. minor* (Karssen et al., 2004) (Table 2): stylet (11.5 µm vs. 9.2 µm) and tail length of J2 (68 µm vs. 54 µm); spicules (35 µm vs. 25.6 µm) and gubernaculum length (8.5 µm vs. 6.1 µm).

Meloidogyne dunensis n. sp. also differs markedly from the other known European root-knot nematodes (Karssen and van Hoenselaar, 1998; Karssen, 2002; Castillo et al., 2003): *M. ardenensis* Santos, 1968; *M. artiellia*

TABLE 2. Morphological and morphometrics differences among *Meloidogyne* species common in European coastal sand dunes[a].

	dunensis n. sp.	*duytsi*	*hapla*	*maritima*	*minor*
			Female		
Stylet length	14 (13–16)	13.3 (12.6–13.9)	15 (13–17)	14.2 (13.9–15.2)	14.2 (12.6–15.2)
Knobs shape	rounded and/or sloping backwards	transversely ovoid	relatively small, rounded and set off	rounded to ovoid, slightly sloping backwards	transversely ovoid, slightly sloping backwards
EP/ST ratio	1.6 (1.2–1.8)	2.8 (2.4–3.4)	3.0	1.1 (0.7–1.2)	1.3 (1.1–1.7)
Perineal pattern	rounded to oval with numerous fine dorsal and ventral striae	asymmetrical shaped, dorsal arch low, with coarse striae	rounded with low dorsal arch, with punctations in tail terminus area	small, rounded to weakly oval, dorsal arch low with coarse striae	small, rounded with fine striae, dorsal arch low with coarse striae
Isozyme[b] phenotype					
Est	VS1	VS1	H1	VS1-S1	VS1
Mdh	N1c	N2	H1	N1c	N1a
			J2		
Body length	446 (417–483)	424 (403–454)	337 (360–500)	471 (442–512)	377 (310–416)
Stylet length	11.5 (11.0–12.5)	11.1 (10.7–12.0)	9.7 (7.9–10.9)	12.4 (12.0–12.6)	9.2 (7.6–10.1)
Hemizonid position	anterior, adjacent to EP	anterior, adjacent to EP	anterior, not adjacent to EP	posterior, not adjacent to EP	posterior, adjacent to EP
Tail length	68 (54–82)	70 (65–77)	(48–70)	72 (66–76)	54 (49–63)
Tail hyaline portion	14.0 (9.5–16.5)	11.3 (9.5–13.3)	(12–19)	13.6 (9.0–17.1)	16.1 (12.0–22.1)
			Male		
Stylet length	20 (16–22)	19.8 (19.0–20.2)	20.5 (19–22)	20.5 (19.6–22.1)	17.8 (17.1–19.0)
Knobs shape	rounded and sloping backwards	transversely ovoid	relatively small, rounded, set off	transversely ovoid	transversely ovoid
Spicules	35 (29–38)	25.9 (24.0–27.2)	25.7 (21.6–28.1)	28.9 (27.8–29.7)	25.6 (22.8–28.4)
Gubernaculum	8.5 (6.0–10.5)	7.1 (6.3–7.6)	8.2 (7.2–9.4)	7.3 (6.3–7.6)	6.1 (5.7–6.3)

[a] All measurements are in µm unless otherwise stated.
[b] Isozyme phenotypes used are defined by Esbenshade and Triantaphyllou (1985).

Franklin, 1961; *M. baetica* Castillo, Vovlas, Subbotin and Troccoli, 2003; *M. fallax* Karssen, 1996; *M. hapla* Chitwood, 1949; *M. hispanica* Hirschmann, 1986; *M. kralli* Jepson, 1983; *M. lusitanica* Abrantes and Santos, 1991; and *M. microtyla* Mulvey, Townshend and Potter, 1975. In addition, *M. dunensis* n. sp. differs from related species in Est and Mdh phenotypes, as well as sequences of the ITS1–5.8S-ITS2 region, the D2-D3 fragment of the 28S gene of rDNA and the small subunit 18S rDNA sequence (see below).

Isozyme and molecular characterization: The isozyme electrophoretic analysis of five-specimen groups of young egg-laying females of *M. dunensis* n. sp. revealed one very slow, weak VS1 Est band after prolonged staining (Fig. 5A) and a N1c Mdh phenotype with two very weak bands (Fig. 5B) that did not occur in the Est and Mdh phenotypes of *M. javanica*, which showed J3 and N1 phenotypes, respectively (Fig. 5).

Amplification of the 18S, ITS1–5.8S-ITS2 and D2-D3 region of 28S rDNA yielded single fragments of approximately 900, 700 and 840 bp, respectively, for *M. dunensis* n. sp. The alignments of the 18S, ITS1–5.8S-ITS2 and D2-D3 region of 28S gene sequences were 780, 580 and 800 bp in length, respectively. The ITS and D2-D3 sequences of *M. dunensis* n. sp. were clearly different from that present in the GenBank database. Substantial sequence divergence for 18S (0.8–3.2%), ITS1–5.8S-ITS2 (10.5–57.2%) and D2-D3 region of 28S (7.5–32.4%) sequences for the new species distinguish *M. dunensis* n. sp. from other studied root-knot nematodes and support its separate specific status (see below).

The topology of the phylogenetic trees obtained with the NJ and MP was consistent, therefore only NJ trees are shown in Figure 6 with bootstrap values. Different *Meloidogyne* spp. were used in the phylogenetic analysis of 18S, ITS1–5.8S-ITS2 and D2-D3 genes due to sequence availability in the GenBank database. For 18S rDNA data, three main clades were identified in the NJ analysis of 18S (Fig. 6A). One clade with low bootstrap support included the most common and widely disseminated species (*M. arenaria*, *M. javanica* and *M. incognita*) plus other *Meloidogyne* spp. (*M. arabicida*, *M. ethiopica*, *M. exigua*, *M. floridensis*, *M. mayaguensis*, *M. morocciensis* and *M. paranaensis*), but the relationships within this clade were poor. Another clade with moderate bootstrap support (62%) included *M. dunensis* n. sp. together with *M. ardenensis*, *M. hapla*, *M. graminis*, *M. maritima*, *M. microtyla* and *M. partityla*. A third,

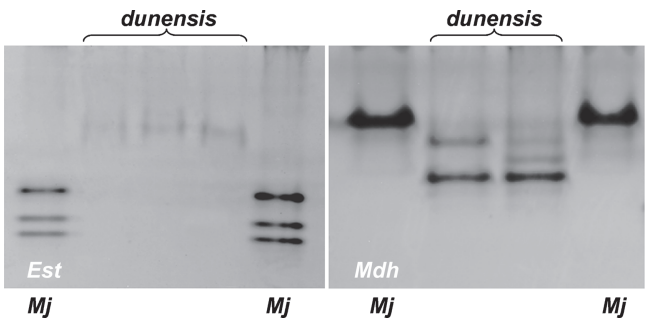

FIG. 5. Esterase (Est) and malate dehydrogenase (Mdh) electrophoresis patterns of protein homogenates from five young, egg-laying females of *Meloidogyne dunensis* n. sp., and five young, egg-laying females of *M. javanica* = reference population.

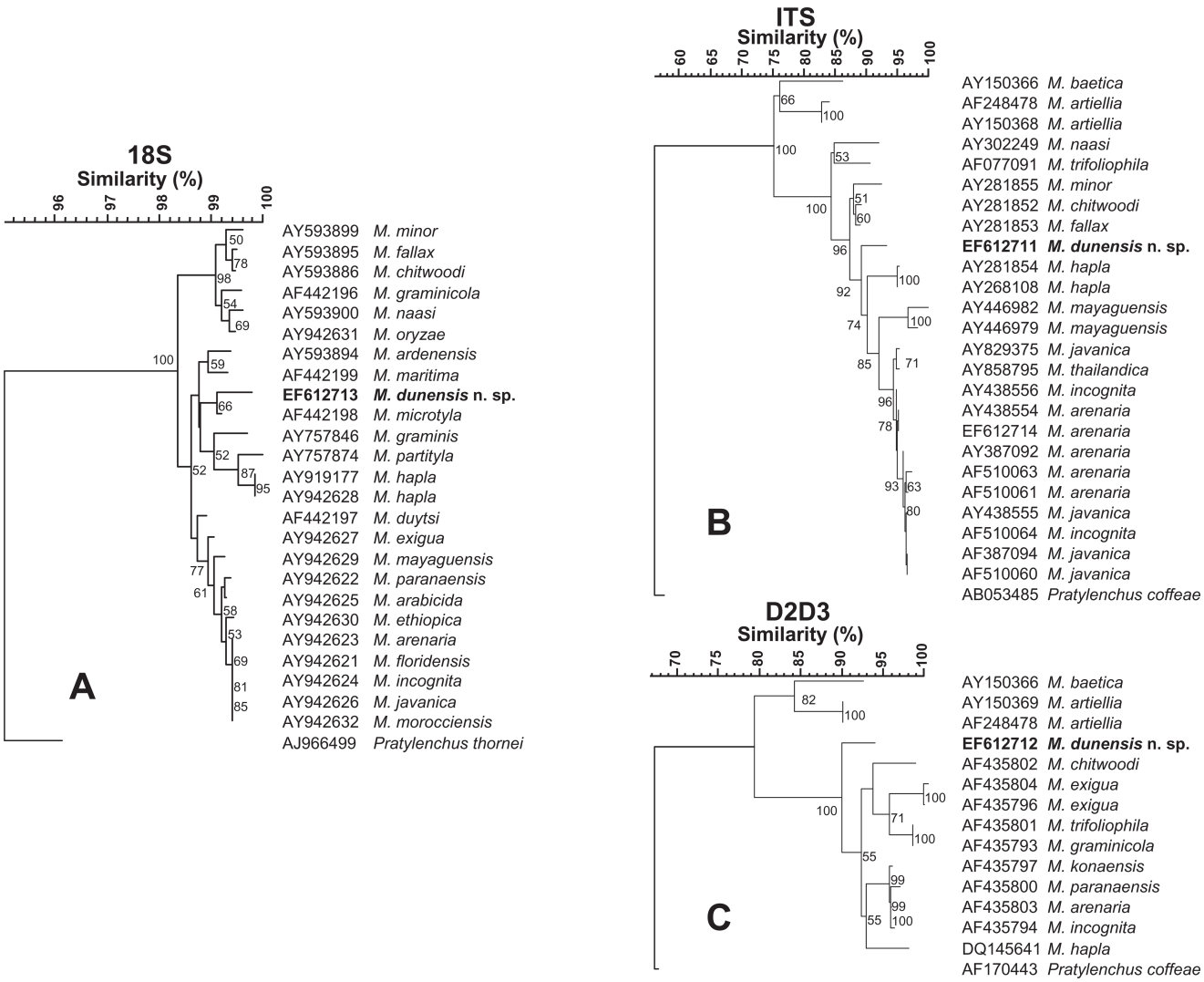

FIG. 6. Rooted Neighbor-Joining trees resulting from analysis of alignments of: A) 18S, B) ITS1–5.8S-ITS2 and C) D2-D3 of 28S of rDNA sequences of *Meloidogyne dunensis* n. sp. with other root-knot nematodes. Bootstrap support more than 50% given for appropriate clade.

highly supported clade (90%) comprised *M. chitwoodi, M. fallax, M. graminicola, M. minor, M. naasi* and *M. oryzae*. The trees obtained from NJ analysis of ITS1–5.8S-ITS2 and D2-D3 sequences showed that *M. dunensis* n. sp. formed a clade with different *Meloidogyne* spp. and maximum bootstrap support (100%) apart from the clade including *M. baetica* and *M. artiellia* (Fig. 6B,C). In the NJ analysis of ITS1–5.8S-ITS2, *M. dunensis* n. sp. (Fig. 6B) appeared occupying a basal position in a clade (92% support) with different *Meloidogyne* spp. such as *M. hapla, M. mayaguensis, M. arenaria, M. javanica, M. thailandica* and *M. incognita* and as a sister taxon (96% support) to *M. minor, M. chitwoodi and M. fallax*; whereas in the NJ analysis of D2-D3 sequences, it stood separately from all the other *Meloidogyne* spp. included in the analysis occupying a basal position within the tree (100% support) (Fig. 6C).

Histopathology: European sea rocket plants, as well as the cultivated hosts (tomato and chickpea), showed similar disease reaction (Figs. 7,8). Root galls induced on the three host roots were variable in size but relatively large (almost three times the root diameter) and located commonly along the root axis but rarely on the root tip. Numerous lateral roots arising from galled root portions were also galled. Frequently, galls containing more than one nematode female were observed associated with their separated feeding sites. Comparative histological observations on healthy and *M. dunensis*-infected European sea rocket, tomato and chickpea roots revealed marked cellular alterations into cortex, endodermis and vascular parenchyma tissues induced by the nematode during its feeding activity. In the permanent feeding sites, the nematode induced a successful formation of large, multinucleate giant cells adjacent to the vascular tissues in all three plant hosts. This formation led to disorganization and disruption of xylem elements and primary phloem cells. Nematode feeding sites comprised three to eight giant cells which surrounded the lip region of a single female (Figs. 7,8).

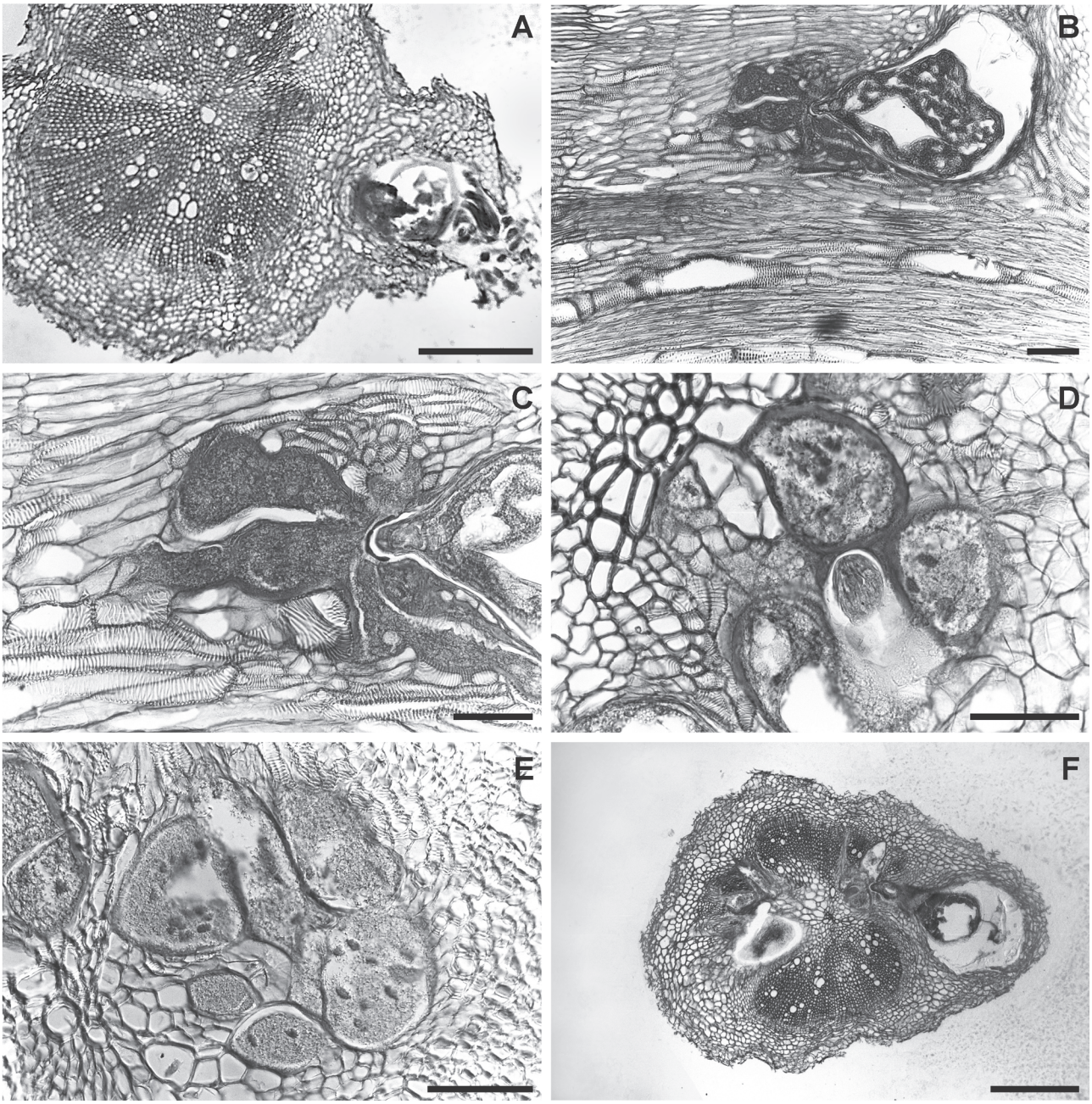

FIG. 7. Infection and feeding site structures of *Meloidogyne dunensis* n. sp. in naturally infected sea rocket roots. A, F) Cross-sections showing nematode infections. B) Longitudinal section. C-E) details of nematode feeding-sites showing multinucleate giant cells with hypertrophied nuclei. Scale bars: A, F = 200 µm; B-E = 100 µm.

Active multinucleated giant cells contained granular cytoplasm, thickened cell wall and numerous hypertrophied nuclei and nucleoli. Dense giant cell cytoplasm lined deeply stained thick walls. The histological modifications induced by *M. dunensis* n. sp. in roots of European sea rocket, tomato and chickpea revealed a typical susceptible reaction to infection by the nematode. The development and parasitic habit of *M. dunensis* n. sp. that we observed in European sea rocket, chickpea and tomato were similar to those reported for *Meloidogyne* spp. on susceptible host plants (Jepson, 1987).

Remarks: Morphology characters and isozyme and molecular analyses have permitted the identification of this new taxon. Although the esterase phenotype of *M. dunensis* n. sp. was similar to that of *M. minor*, which also revealed a single VS1 band at a similar position (Karssen et al., 2004) but different to that of *M. maritima* which shows an Est VS1-S1 phenotype (Karssen et al., 1998), the Mdh phenotype of *M. dunensis* n. sp. was similar to that of *M. maritima* but clearly different than that of *M. minor*, which revealed an N1a phenotype with two additional weaker bands after prolonged staining (Karssen et al., 2004). Similarly, isozyme electrophoretic phenotypes of *M. dunensis* sp. n. were different

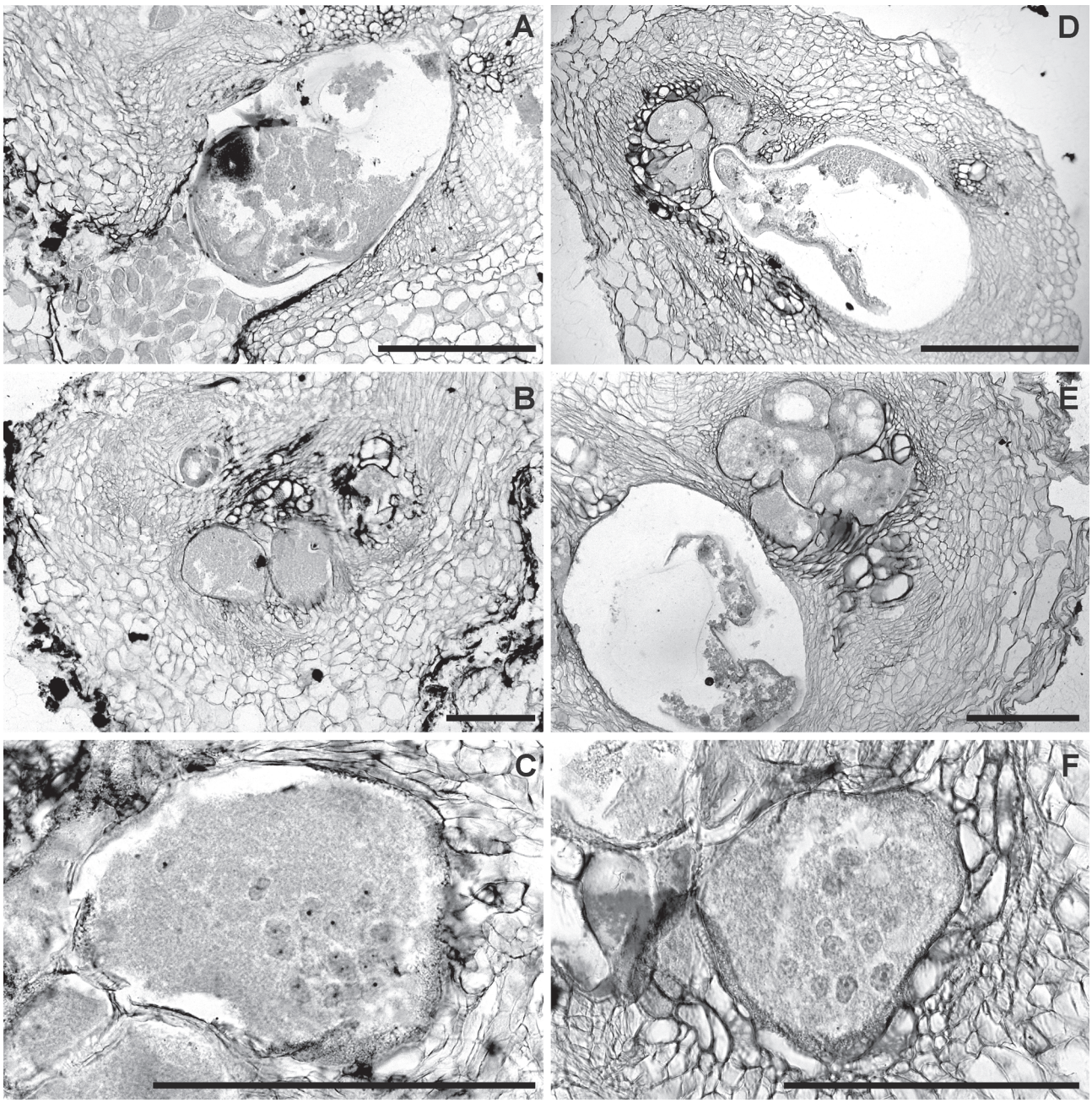

FIG. 8. Histopathology of *Meloidogyne dunensis* n. sp. in artificially infected roots of: A-C) Tomato (cv. Roma). D-F) chickpea (cv. UC 27) showing multinucleate giant cells with hypertrophied nuclei. Scale bars = 200 µm.

from those of other root-knot nematodes showing resemblance in morphology. Also, the isozyme electrophoretic phenotype of *M. ardenensis* is characterized by a faint multiple banding Est phenotype and an N1a type Mdh phenotype (Karssen, 2002), and *M. mayaguensis* shows a VS1-S1 phenotype of Est with two major bands and an N1a Mdh phenotype with one strong band (Brito et al., 2004). Finally, *M. duytsi* is characterized by a VS1 Est pattern and an N2 Mdh pattern (Table 2), which clearly differs from that of *M. dunensis* n. sp. (Karssen et al., 1998).

The trees obtained from NJ analysis of different rDNA sequences agreed with those obtained in similar analysis by Castillo et al. (2003) and Tigano et al. (2005). The addition of the sequences of this new species or different or additional sequences from GenBank database to the distance and maximum parsimony analyses caused small subtle changes in topology of the dendrograms shown in Figure 6 compared to that reported previously (Castillo et al., 2003; Tigano et al., 2005). NJ and MP analysis showed that 18S, ITS1–5.8S-ITS2 and D2-D3 sequences of *M. dunensis* n. sp. present enough divergence to differentiate *M. dunensis* n. sp. from other species with resemblance in morphology, such as *M. duytsi*, *M. maritima*, *M. mayaguensis* and *M. minor*.

Literature Cited

Abolafia, J., Liebanas, G., and Peña-Santiago, R. 2002. Nematodes of the order Rhabditida from Andalucia Oriental, Spain. The subgenus *Pseudacrobeles* Steiner, 1938, with description of a new species. Journal of Nematode Morphology and Systematics 4:137–154.

Abrantes, I. M. D. O., and Santos, M. S.N. de A. 1991. *Meloidogyne lusitanica* n. sp. (Nematoda: Meloidogynidae), a root-knot nematode parasitizing olive tree (*Olea europaea* L.). Journal of Nematology 23: 210–224.

Blok, V.C. 2005. Achievements in and future prospects for molecular diagnostics of plant-parasitic nematodes. Canadian Journal of Plant Pathology 27:176–185.

Blok, V. C., Phillips, M. S., and Fargette, M. 1997. Comparison of sequences from the ribosomal DNA intergenic region of *Meloidogyne mayaguensis* and other major tropical root-knot nematodes. Journal of Nematology 29:16–22.

Blok, V. C., Wishart, J., Fargette, M., Berthier, K., and Phillips, M. S. 2002. Mitochondrial DNA differences distinguishing *Meloidogyne mayaguensis* from the major species of tropical root-knot nematodes. Nematology 4:773–781.

Brito, J., Powers, T. O., Mullin, P. G., Inserra, R. N., and Dickson, A. W. 2004. Morphological and molecular characterization of *Meloidogyne mayaguensis* isolates from Florida. Journal of Nematology 36:232–240.

Castillo, P., Vovlas, N., Subbotin, S., and Troccoli, A. 2003. A new root-knot nematode, *Meloidogyne baetica* n. sp. (Nematoda: Heteroderidae), parasitizing wild olive in Southern Spain. Phytopathology 93: 1093–1102.

Chen, P., Roberts, P. A., Metcalf, A. E., and Hyman, B. C. 2003. Nucleotide substitution patterning within the *Meloidogyne* rDNA D3 region and its evolutionary implications. Journal of Nematology 35: 404–410.

Coolen, W. A. 1979. Methods for extraction of *Meloidogyne* spp. and other nematodes from roots and soil. Pp. 317–329 *in* F. Lamberti and C. E. Taylor, eds. Root-knot nematodes (*Meloidogyne* species). Systematics, biology, and control. New York: Academic Press.

De Ley, P., and Blaxter, M. L. 2002. Systematic position and phylogeny. Pp. 1–30 *in* D. L. Lee, ed. The Biology of Nematodes. London, UK: Taylor and Francis.

Eisenback, J. D., and Triantaphyllou, H. H. 1991. Root-knot nematodes: *Meloidogyne* species and races. Pp. 191–274 *in* W. R. Nickle, ed. Manual of Agricultural Nematology. New York: Marcel Dekker.

Esbenshade, P. R., and Triantaphyllou, A. C. 1985. Use of enzyme phenotypes for identification of *Meloidogyne* species. Journal of Nematology 17:6–20.

Esser, R. P. 1986. A water agar en face technique. Proceedings of the Helminthological Society of Washington 53:254–255.

Hartman, K. M., and Sasser, J. N. 1985. Identification of *Meloidogyne* species on the basis of differential host assay and perineal-pattern morphology. Pp. 67–77 *in* K. R. Barker, C. C. Carter, and J. N. Sasser, eds. An Advanced Treatise on Meloidogyne. Vol. II. Methodology. Raleigh, North Carolina: North Carolina State University Graphics.

Hugall, A., Moritz, C., Stanton, J., and Wolstenholmes, D. R. 1994. Low, but strongly structured mitochondrial DNA diversity in root knot nematodes (*Meloidogyne*). Genetics 136:903–912.

Hussey, R. S., and Barker, K. R. 1973. A comparison of methods of collecting inocula of *Meloidogyne* spp. including a new technique. Plant Disease Reporter 57:1025–1028.

Jepson, S. B. 1987. Identification of root-knot nematodes (*Meloidogyne* species). Wallingford, UK: CABI.

Johansen, D. A. 1940. Plant Microtechnique. New York: McGraw-Hill.

Karssen, G. 2002. The plant-parasitic nematode genus *Meloidogyne* Göldi, 1892 (Tylenchida) in Europe. Leiden, The Netherlands: Brill Academic Publishers.

Karssen, G., Bolk, R. J., van Aelst, A. C., van den Beld, I., Kox, L. F. F., Korthals, G., Molendijk, L., Zijlstra, C., van Hoof, R., and Cook, R. 2004. Description of *Meloidogyne minor* n. sp. (Nematoda: Meloidogynidae), a root-knot nematode associated with yellow patch disease in golf courses. Nematology 6:59–72.

Karssen, G., and Moens, M. 2006. Root-knot nematodes. Pp. 59–90 *in* R. N. Perry, and M. Moens, eds. Plant Nematology. Wallingford, UK: CABI Publishing.

Karssen, G., van Aelst, A., and Cook, R. 1998. Redescription of the root-knot nematode *Meloidogyne maritima* Jepson, 1987 (Nematoda: Heteroderidae), a parasite of *Ammophila arenaria* (L.) Link. Nematologica 44:241–253.

Karssen, G., and van Hoenselaar, T. 1998. Revision of the genus *Meloidogyne* Göldi, 1892 (Nematoda: Heteroderidae) in Europe. Nematologica 44:713–788.

Nico, A. I., Jiménez-Díaz, R. M., and Castillo, P. 2003. Host suitability of the olive cultivars Arbequina and Picual for plant-parasitic nematodes. Journal of Nematology 35:29–34.

Seinhorst, J. W. 1966. Killing nematodes for taxonomic study with hot f.a. 4:1. Nematologica 12:178.

Siddiqi, M. R. 2000. Tylenchida parasites of plants and insects. 2nd edition. Wallingford, UK: CABI Publishing.

Tigano, M. S., Carneiro, R. M. D. G., Jeyaprakash, A., Dickson, D. W., and Adams, B. J. 2005. Phylogeny of *Meloidogyne* spp. based on 18S rDNA and the intergenic region of mitochondrial DNA sequences. Nematology 7:851–862.

Wishart, J., Phillips, M. S., and Blok, V. C. 2002. Ribosomal intergenic spacer: A polymerase chain reaction diagnostic for *Meloidogyne chitwoodi*, *M. fallax*, and *M. hapla*. Phytopathology 92:884–892.

Zijlstra, C., Donkers-Venne, D. T. H. M., and Fargette, M. 2000. Identification of *Meloidogyne incognita, M. javanica* and *M. arenaria* using sequence characterized amplified region (SCAR) based PCR assays. Nematology 2:847–853.